

A NEW EINSTEIN CROSS: A HIGHLY MAGNIFIED, INTRINSICALLY FAINT LYMAN-ALPHA EMITTER AT $Z = 2.7$

ADAM S. BOLTON¹, LEONIDAS A. MOUSTAKAS², DANIEL STERN², SCOTT BURLES³, ARJUN DEY⁴, AND HYRON SPINRAD⁵
ApJ Letters, in press

ABSTRACT

We report the discovery of a new Einstein cross at redshift $z_S = 2.701$ based on Ly α emission in a cruciform configuration around an SDSS luminous red galaxy ($z_L = 0.331$). The system was targeted as a possible lens based on an anomalous emission line in the SDSS spectrum. Imaging and spectroscopy from the W.M. Keck Observatory confirm the lensing nature of this system. This is one of the widest-separation galaxy-scale lenses known, with an Einstein radius $\theta_E \simeq 1.84$ arcsec. We present simple gravitational lens models for the system and compute the intrinsic properties of the lensed galaxy. The total mass of the lensing galaxy within the 8.8 ± 0.1 kpc enclosed by the lensed images is $(5.2 \pm 0.1) \times 10^{11} M_\odot$. The lensed galaxy is a low mass galaxy ($0.2 L_*$) with a high equivalent-width Ly α line ($EW_{\text{Ly}\alpha}^{\text{rest}} = 46 \pm 5$ Å). Follow-up studies of this lens system can probe the mass structure of the lensing galaxy, and can provide a unique view of an intrinsically faint, high-redshift, star-forming galaxy at high signal-to-noise ratio.

Subject headings: gravitational lensing — galaxies: elliptical, starburst, high-redshift — techniques: spectroscopic — galaxies: individual (SDSS J101129.49+014323.3)

1. INTRODUCTION

Strong gravitational lensing is a powerful tool for the measurement of lensing galaxy masses and for the detailed study of magnified high-redshift sources. Multiple lensed images can directly constrain models for the distribution of mass in the lens on the scale of the Einstein radius θ_E . In well-studied cases, these observations directly test theories for the central dark-matter profile in both galaxies (e.g., Koopmans & Treu 2003; Dye & Warren 2005) and galaxy clusters (e.g., Kneib et al. 1995, 1996; Abdelsalam, Saha, & Williams 1998a,b). Simultaneously, lensed background galaxies can be magnified by factors of up to several tens, providing data of a quality which would not otherwise be possible. Such data have been used to constrain the faint end of the high-redshift galaxy luminosity function (e.g., Santos et al. 2004), study distant galaxies at wavelengths which would be impractical without magnification (e.g., Chary, Stern, & Eisenhardt 2005), and probe detailed properties of high-redshift galaxies (Pettini et al. 2002).

Systematic searches for new galaxy-scale strong gravitational lenses are traditionally based on imaging detections (e.g., Maoz et al. 1993; Gregg et al. 2000; Wisotzki et al. 2002; Inada et al. 2003; Morgan et al. 2003; Richards et al. 2004; Pindor et al. 2004), although a handful of lenses have been identified in spectroscopic observations (Huchra et al. 1985; Warren et al.

1996; Johnston et al. 2003). The Sloan Lens ACS (SLACS) survey (Bolton et al. 2006; Treu et al. 2006; Koopmans et al. 2006) efficiently identifies new gravitational lenses by searching the spectroscopic database of the Sloan Digital Sky Survey (SDSS; York et al. 2000) for systems consisting of low-redshift ($z \sim 0.1$ – 0.4) luminous elliptical galaxies superposed with moderate-redshift ($z \sim 0.3$ – 1) star-forming galaxies (see also Bolton et al. 2004, Willis, Hewett, & Warren 2005, and Willis et al. 2006). This technique relies upon the detection of *multiple* anomalous nebular emission lines in the SDSS fiber spectra of lensing early-type galaxies. In principle, the anomalous emission line technique can also identify lenses with higher redshift, Ly α -emitting source galaxies (Warren et al. 1996; Hewett et al. 2000; Willis 2000). In practice this approach has been less productive because strong, high-redshift Ly α emitters are less numerous on the sky than moderate-redshift galaxies showing oxygen and Balmer emission lines to the SDSS line-flux limits, and the increase in lensing cross section with source redshift does not overcome this effect.

This *Letter* reports the discovery of a new spectroscopically-selected strong gravitational lens with a Ly α -emitting galaxy as its source, SDSS J101129.49+014323.3 (hereafter J1011+0143). The lensed galaxy forms a highly symmetric Einstein cross which, by virtue of its large physical scale, provides leverage for determining the dark-matter halo mass of the lensing elliptical. The system also provides a highly magnified view of an intrinsically faint, compact, and high-redshift star-forming galaxy.

For all calculations, we assume a universe with $(\Omega_M, \Omega_\Lambda, h) = (0.3, 0.7, 0.7)$.

2. DISCOVERY AND CONFIRMATION

J1011+0143 was discovered on the basis of an anomalous emission line in its SDSS spectrum at a vacuum wavelength of 4500 Å (see Fig. 1). Table 1 provides parameters for the system as determined from the SDSS

arXiv:astro-ph/0606210v1 8 Jun 2006

¹ Harvard-Smithsonian Center for Astrophysics, 60 Garden St., Cambridge, MA 02138 (abolton@cfa.harvard.edu)

² Jet Propulsion Laboratory, California Institute of Technology, 4800 Oak Grove Drive, Pasadena, CA 91109 (leonidas@jpl.nasa.gov, stern@thisvi.jpl.nasa.gov)

³ Department of Physics and Kavli Institute for Astrophysics and Space Research, Massachusetts Institute of Technology, 77 Massachusetts Avenue, Cambridge, MA 02139 (burles@mit.edu)

⁴ National Optical Astronomy Observatory, 950 N. Cherry Ave., Tucson, AZ 85719 (dey@noao.edu)

⁵ Department of Astronomy, UC-Berkeley, Berkeley, CA 94720 (spinrad@astron.berkeley.edu)

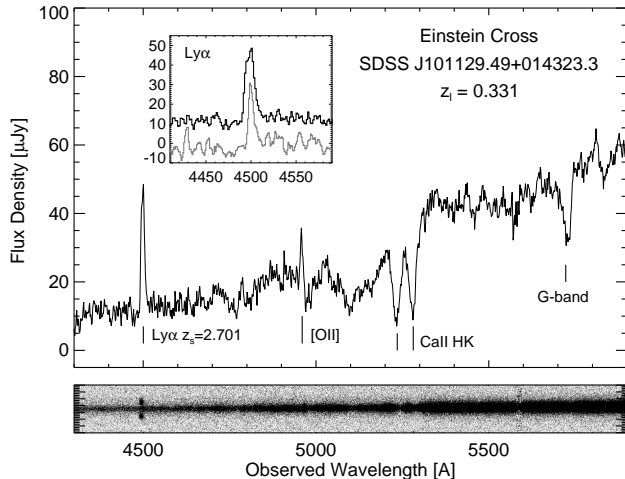


FIG. 1.— Spectrum of J1011+0143 (one-dimensional and two-dimensional forms), obtained with Keck/LRIS on UT 2004 Nov 10, with features indicated. The spectrum was obtained through a $1''.5$ slit aligned with the minor axis of the lensing galaxy. The 1D spectrum has been scaled to match the spectrophotometry of the lensing elliptical. Ly α detail window also shows the SDSS line detection (grey), smoothed by 5 pixels and shifted downwards by $20 \mu\text{Jy}$. Note the appearance of the lensed Ly α line on either side of the lensing galaxy continuum in the 2D spectrum.

data. The system was one of several single-line lens candidates selected from the luminous red galaxy (LRG) sample of the SDSS (Eisenstein et al. 2001). These candidates were identified by subtracting best-fit galaxy spectrum templates from the SDSS spectra of the LRGs, and then searching for significant ($\geq 7\sigma$) residual emission. The search was done via convolution with a Gaussian kernel matched to the SDSS spectral resolution ($\approx 150 \text{ km s}^{-1}$). Spectrum noise estimates were empirically rescaled in a manner similar to that of Bolton et al. (2004). Our search was confined to wavelengths shortward of 6500 \AA since at redder wavelengths one must contend with a deluge of low-redshift H α detections. Candidates were subjected to several pruning steps to reject (1) unmodeled LRG rest-frame absorption/emission, (2) night-sky emission residuals, (3) spectra of very poor data quality, (4) line profiles narrower than the SDSS spectral resolution, and (5) lines other than Ly α as judged by multiple emission lines at the same redshift. In preparation for a single observing run, 21 priority candidates were identified in the ranges 19h–01h and 05h–11h. SDSS imaging of these candidates was inspected to verify the absence of bright neighboring galaxies that could account for anomalous emission lines.

In order to confirm the SDSS anomalous emission line detection, initial follow-up of J1011+0143 was conducted on the night of UT 2004 November 9 using the Low Resolution Imaging Spectrometer (LRIS; Oke et al. 1995) with the Keck I Telescope. A large slit of $1''.5$ width was used to maximize the aperture with which to detect any lensed emission-line flux. The slit, which is still smaller than the $3''$ diameter fibers used in the discovery SDSS spectroscopy, was aligned with the parallactic angle. The exposure time was 10 min and conditions were photomet-

TABLE 1
SDSS PARAMETERS FOR J1011+0143

SDSS ID ^a	J2000 RA ^b	J2000 Dec. ^b
502-51957-172	10h11m29.50s	+01d43m23.4s

g, r, i [AB] ^c	R_{eff} ["] ^d	z_{lens}	z_{source}	σ_v [km s ⁻¹] ^e
19.4, 18.1, 17.5	1.71 ± 0.1	0.3308	2.701	259 ± 16

- a: SDSS PLATE-MJD-FIBERID (MJD = modified Julian date)
b: Coordinates accurate to $0''.1$
c: Extinction-corrected DeVaucouleurs model magnitudes.
d: Effective radius at intermediate axis.
e: Stellar velocity dispersion as measured from SDSS spectroscopy.

ric with $0''.8$ seeing. The two-dimensional spectrum of J1011+0143 showed extended emission-line morphology at the wavelength of the SDSS detection (4500 \AA). Three other candidate systems observed similarly on the same night showed no evidence of the line emission detected by SDSS, and hence are presumed associated with noise or cosmic rays in the SDSS spectroscopy⁶. Based on the confirmation of the SDSS line emission, J1011+0143 was observed again on the night of UT 2004 November 10 with LRIS B -band (600 s) and I -band (420 s) imaging, as well as further, deeper (30 min) spectroscopy. The B -band image shows a distinctive quadruple-image cross morphology, aligned with the principal axes of the LRG and characteristic of strong gravitational lensing (Fig. 2). For the additional spectroscopy, the $1''.5$ slit was aligned with the minor axis of the LRG. The resulting spectrum is shown in Fig. 1.

Although based on a single emission line, the identification of the cross emission line at 4500 \AA with redshifted Ly α is secure for the following reasons. First, the Keck detections confirm that the emission line is real and not an artifact or night-sky residual. Second, the spectroscopic data (particularly the higher resolution SDSS detection) show the classic, asymmetric, self-absorbed morphology typical of Ly α emission. Third, the wavelength of the line does not correspond to any common emission wavelength at the redshift of the LRG. Finally, the only other possible common emission lines observable at 4500 \AA are [O II] $\lambda 3727$ or Balmer lines of order H γ and higher. The [O II] identification is strongly disfavored by both the line morphology and the absence of corresponding [O III] and H α emission. A Balmer-series identification is likewise disfavored by the absence of other Balmer-series lines.

3. IMAGE ANALYSIS AND LENS MODELING

The four symmetrically-arranged lensed images are well-detected in the Keck B -band image (Fig. 2). Even with a B -band seeing of $1''$, we can successfully fit simple analytic models given the wide image separation. We measure relative positions of the lensed images with re-

⁶ The three non-detections are identified by the following SDSS PLATE-MJD-FIBERID values, with J2000 right ascensions and declinations and anomalous line wavelengths given parenthetically: 385-51877-437 (23h39m24.33s +00d32m34.2s, 5116 \AA); 389-51795-373 (00h12m49.09s +00d53m21.9s, 6180 \AA); and 656-52148-411 (00h44m52.11s -09d04m54.6s, 4302 \AA).

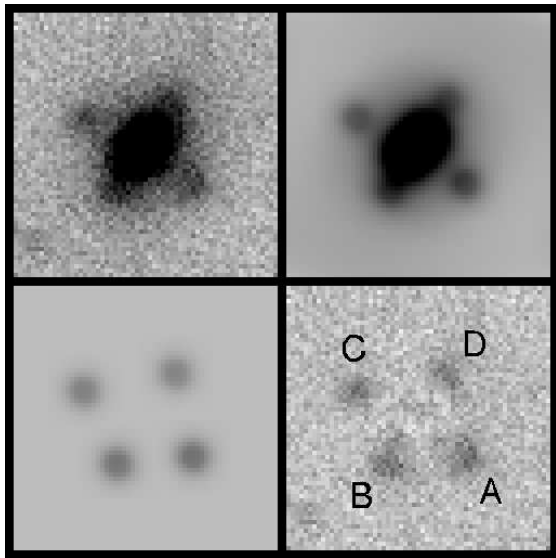


FIG. 2.— B -band data, model, and residual images of J1011+0143. Shown from upper left to lower right are direct image, composite model, lensed-image model and galaxy model-subtracted residual. Image region is $8''.2 \times 8''.2$, with north up and east to the left.

TABLE 2
MEASURED PARAMETERS OF B -BAND IMAGE COMPONENTS

Image	$\Delta\alpha$ ("E) ^a	$\Delta\delta$ ("N) ^a	Magnitude (B_{AB}) ^b
G	$\equiv 0$	$\equiv 0$	19.86 ± 0.01
A	-1.55 ± 0.02	-1.14 ± 0.02	23.79 ± 0.04
B	$+0.81 \pm 0.03$	-1.36 ± 0.03	23.84 ± 0.04
C	$+1.86 \pm 0.03$	$+0.91 \pm 0.03$	24.05 ± 0.05
D	-1.00 ± 0.03	$+1.46 \pm 0.04$	24.10 ± 0.05

^a: Positions relative to Table 1 coordinates.

^b: Quoted uncertainties do not include overall magnitude zeropoint uncertainty of ≈ 0.1 .

spect to the lensing galaxy by fitting a model composed of four PSFs (for the four lensed images) and a radial b-spline with a quadrupole angular dependence (for the lens galaxy; see Bolton et al. 2006 for a full discussion of radial b-splines). Table 2 gives the parameters of the derived image components. We fit over an image cutout of $61 \times 61 = 6721$ pixels, subtending a region $8''.2$ on a side. The composite image model has a total of 38 free parameters, and the χ^2 per degree of freedom of the fit is $\chi^2_R = 1.21$. Fig. 2 shows data, model, and residual images of the fitted region about the lens. The model implies a flux ratio of 10.77 between the total B -band flux of the lensing galaxy and the summed flux of the four lensed images.

The lensed images are not readily visible in the I -band Keck image. This is likely due to a combination of the intrinsic faintness of the lensed images at this wavelength and the red color of the lensing elliptical. In addition, b-spline galaxy subtraction of the I -band image is complicated by an asymmetric PSF. For these reasons, no quantitative analysis of the I -band image is presented.

Given the limited spatial resolution and signal-to-noise

TABLE 3
LENS MODEL PARAMETERS

Model parameter	SIE no shear	SIS plus shear
b (arcsec)	1.87 ± 0.02	1.84 ± 0.02
b (kpc)	8.9 ± 0.1	8.8 ± 0.01
Quadrupole	$q = 0.77 \pm 0.03$ $\gamma = 0.078 \pm 0.008$	
PA ($^\circ$ E of N)	148.4 ± 0.1	148.4 ± 0.1
Rel. Lens RA ("E) ^a	-0.03 ± 0.02	-0.01 ± 0.02
Rel. Lens Dec. ("N) ^a	$+0.10 \pm 0.02$	$+0.09 \pm 0.02$
Rel. Source RA ("E) ^a	$+0.01 \pm 0.02$	$+0.02 \pm 0.02$
Rel. Source Dec. ("N) ^a	$+0.07 \pm 0.02$	$+0.06 \pm 0.02$
Source Magnitude (B_{AB}) ^b	25.9 ± 0.1	26.0 ± 0.1
Total Magnif.	23 ± 3	26 ± 2
χ^2 (d.o.f.)	61.1(4)	23.2(4)
$\chi^2_{\text{posn}}, \chi^2_{\text{flux}}$	35.4, 25.7	10.9, 12.3
Lens-model vdisp. (km s ⁻¹)	288 ± 2	285 ± 2
Mass within b ($10^{11} M_\odot$)	5.4 ± 0.1	5.2 ± 0.1

^a: Positions relative to Table 1 coordinates.

^b: Best-fit lens model parameter value for unlensed point-source magnitude.

ratio of our current data, we consider only a standard singular isothermal ellipsoid (SIE) lens model and a singular isothermal sphere with external shear (SIS γ). Both models are simple, analytic, physically motivated and free from severe parameter degeneracies. The angular Einstein radius b of the SIS model is related to the velocity dispersion σ of the lensing distribution through $b_{\text{SIS}} = 4\pi(\sigma^2/c^2)(D_{\text{LS}}/D_{\text{S}})$, where D_{LS} and D_{S} are angular-diameter distances from lens to source and observer to source. To assign a lensing velocity dispersion to an SIE model with minor-to-major axis ratio $q < 1$, we adopt the intermediate-axis normalization of Kormann, Schneider, & Bartelmann (1994), whereby the mass interior to a given is-density contour at fixed b is constant with changing q .

The data provide 12 constraints (RA, Dec., and flux for each of the four lensed images). We implement both SIE and SIS γ models with a total of 8 free parameters. The best-fit (minimum- χ^2) values for these parameters are determined using custom IDL routines that invoke the MPFIT implementation of the Levenberg-Marquardt minimization algorithm (Moré & Wright 1993). Table 3 gives fitted values of the parameters for both models. Although the alignment of the four lensed images with the principal axes of the LRG suggest that the intrinsic ellipticity of the lens galaxy is responsible for the quadrupole of the lensing potential, the SIS γ model provides a better fit than the SIE to both the image positions and fluxes. We note that using image fluxes as lens-model constraints is a legitimate tactic, given that the source is likely to be a small but extended high-redshift star-forming galaxy, and thus immune to both the microlensing perturbations and temporal variability that affect lensed quasar image fluxes. Large-mass substructures in the lens could, however, perturb the image fluxes from the predictions of smooth models.

Adopting $b = 1.84 \pm 0.02$ from the best-fit SIS γ model, the mass enclosed by the lensed images is $(5.2 \pm 0.1) \times 10^{11} M_\odot$. The corresponding lensing velocity dispersion

is $\sigma_{\text{SIS}} = 285 \pm 2 \text{ km s}^{-1}$. This is larger than the stellar value from the SDSS spectrum of $\sigma_v = 259 \pm 16 \text{ km s}^{-1}$ (based on a median SNR per pixel of 10 and a resolution of $\approx 150 \text{ km s}^{-1}$), although the significance of the difference is less than two standard deviations. The Keck spectroscopic data do not permit an independent determination of the stellar velocity dispersion due to their lower resolution ($\approx 600 \text{ km s}^{-1}$).

4. PROPERTIES OF THE LENSED GALAXY

The Ly α flux in each of the cross components observed on UT 2004 November 10 is $2.8 \times 10^{-16} \text{ erg cm}^{-2} \text{ s}^{-1}$. For all four lensed components having roughly equal Ly α flux, the implied total Ly α flux for the Einstein cross is $1.1 \times 10^{-15} \text{ erg cm}^{-2} \text{ s}^{-1}$. For our assumed cosmology and the magnification of the best-fit SIS γ model, we derive an intrinsic Ly α luminosity of $2 \times 10^{42} \text{ erg s}^{-1}$. Dawson et al. (2006) present the most recent, comprehensive derivation of the luminosity function of high-redshift Ly α emitters. They conclude that $L_* \approx 10 \times 10^{42} \text{ erg s}^{-1}$, with no evidence for evolution in the Ly α luminosity function between $z \approx 3$ and $z \approx 6$. This implies that J1011+0143 is an intrinsically faint Ly α emitter, with a luminosity $\approx 0.2L_*$, but with a magnification that makes it among the brightest high-redshift Ly α emitters known.

The current Keck spectroscopy is of insufficient depth to allow detection of the faint continuum of the lensed galaxy. We thus combine SDSS photometry (Table 1, assuming statistical errors of 0.1 mag) and Keck imaging and spectroscopy to estimate the broadband magnitude and Ly α equivalent width of the lensed galaxy. We assume the shape of the lens galaxy continuum to be given by the best-fit template spectrum from the Princeton SDSS redshift pipeline⁷. For the lensed galaxy, we assume a simple model for the continuum shape that includes Ly α forest absorption:

$$f_\nu(\lambda) = \begin{cases} f_{\text{cont}}, & \lambda/(1+z_s) > 1216\text{\AA}; \\ 0.55f_{\text{cont}} & 1026 < \lambda/(1+z_s) \leq 1216\text{\AA}. \end{cases} \quad (1)$$

This model is a reasonable approximation to the composite spectrum of the strongest Ly α -emitting LBGs at similar redshifts published by Shapley et al. (2003). We integrate these continuum models over g and B filter curves, together with the known contribution from the measured Ly α line flux. We then deduce the relative normalization of each continuum component from (1) the measured SDSS g band flux for the entire system, and (2) the measured Keck B -band flux ratio of 10.77 of the lens to the source (continuum plus line, summed over all four lensed images). The results give $B_{\text{AB,lens}} = 19.9 \pm 0.1$ and $B_{\text{AB,source}} = 22.5 \pm 0.1$. Taking the total magnification of the best-fit SIS γ model, we find an unlensed magnitude for the source galaxy of $B_{\text{AB,source}}^{\text{unlensed}} = 26.0 \pm 0.1$. The implied continuum flux density of the lensed galaxy red-ward of Ly α (including the observed magnification) is $4.3 \pm 0.4 \mu\text{Jy}$, giving an observed equivalent width of $EW_{\text{Ly}\alpha}^{\text{obs}} = 170 \pm 20 \text{\AA}$. Correcting for cosmological expansion, this becomes $EW_{\text{Ly}\alpha}^{\text{rest}} = 46 \pm 5 \text{\AA}$, a value typical of confirmed high-redshift Ly α emitters (e.g., Dawson et al. 2006).

5. SUMMARY AND CONCLUSIONS

We present the discovery of a new high-redshift Einstein-cross gravitational lens, J1011+0143. The lens galaxy is a bright elliptical at $z_{\text{lens}} = 0.331$, while the lensed source is a $\sim 0.2L_*$ Ly α -bright, star-forming galaxy at redshift $z_{\text{source}} = 2.701$. Though such high- z Ly α lenses appear to be much less numerous in the SDSS than lenses with lower redshift ($z \lesssim 1$) oxygen- and Balmer-line emitting sources (Bolton et al. 2004; Willis et al. 2005; Bolton et al. 2006; Willis et al. 2006), the discovery of J1011+0143 demonstrates their presence. Depending on the luminosity function slope of the Ly α -emitting source population, deeper spectroscopic surveys could yield an appreciable sample of such lens systems.

As with all gravitational lenses, this system offers a powerful tool for measuring the mass in the lensing galaxy. J1011+0143 is of particular interest for its relatively wide ($\sim 4''$) image separation, probing the lens galaxy at a radius within which the contributions of luminous and dark matter are expected to be comparable. As with the sample of lenses discovered by the SLACS survey (Bolton et al. 2006), the image of the lens galaxy is not overwhelmed by lensed-quasar images and is thus accessible to accurate photometric and dynamical observations. The high degree of symmetry of the image configuration suggests that a largely model-independent test of the relative degree of flattening between the mass and light distributions in the early-type lens galaxy will be enabled by high-resolution imaging. A modest Cycle 15 *HST*/ACS program to image this system has been awarded two orbits (P.I. Moustakas).

J1011+0143 also offers a highly magnified view of a sub- L_* starforming galaxy at high redshift. This discovery is thus complementary to the more luminous Lyman-break galaxy MS1512-cB15 (Yee et al. 1996), which is also strongly magnified by gravitational lensing (Seitz et al. 1998). The magnification of J1011+0143 suggests this system as a target for deep spectroscopic studies of the high-redshift IGM that would otherwise be infeasible due to the intrinsic source faintness.

Some of the data presented herein were obtained at the W.M. Keck Observatory, which is operated as a scientific partnership among the California Institute of Technology, the University of California and the National Aeronautics and Space Administration. The Observatory was made possible by the generous financial support of the W.M. Keck Foundation. The authors wish to recognize and acknowledge the very significant cultural role and reverence that the summit of Mauna Kea has always had within the indigenous Hawaiian community; we are most fortunate to have the opportunity to conduct observations from this mountain. The work of LAM and DS was carried out at Jet Propulsion Laboratory, California Institute of Technology, under a contract with NASA. AD acknowledges support from NOAO, which is operated by the Association of Universities for Research in Astronomy (AURA), Inc. under a cooperative agreement with the National Science Foundation.

⁷ <http://spectro.princeton.edu>

REFERENCES

- Abdelsalam, H. M., Saha, P., & Williams, L. L. R. 1998a, *MNRAS*, 294, 734
- . 1998b, *AJ*, 116, 1541
- Bolton, A. S., Burles, S., Koopmans, L. V. E., Treu, T., & Moustakas, L. A. 2006, *ApJ*, 638, 703
- Bolton, A. S., Burles, S., Schlegel, D. J., Eisenstein, D. J., & Brinkmann, J. 2004, *AJ*, 127, 1860
- Chary, R.-R., Stern, D., & Eisenhardt, P. 2005, *ApJ*, 635, L5
- Dawson, S., et al. 2006, in preparation
- Dye, S., & Warren, S. J. 2005, *ApJ*, 623, 31
- Eisenstein, D. J., et al. 2001, *AJ*, 122, 2267
- Gregg, M. D., Wisotzki, L., Becker, R. H., Maza, J., Schechter, P. L., White, R. L., Brotherton, M. S., & Winn, J. N. 2000, *AJ*, 119, 2535
- Hewett, P. C., Warren, S. J., Willis, J. P., Bland-Hawthorn, J., & Lewis, G. F. 2000, in *ASP Conf. Ser. 195: Imaging the Universe in Three Dimensions*, 94
- Huchra, J., Gorenstein, M., Kent, S., Shapiro, I., Smith, G., Horine, E., & Perley, R. 1985, *AJ*, 90, 691
- Inada, N., et al. 2003, *AJ*, 126, 666
- Johnston, D. E., et al. 2003, *AJ*, 126, 2281
- Kneib, J.-P., Ellis, R. S., Smail, I., Couch, W. J., & Sharples, R. M. 1996, *ApJ*, 471, 643
- Kneib, J. P., Mellier, Y., Pello, R., Miralda-Escude, J., Le Borgne, J.-F., Boehringer, H., & Picat, J.-P. 1995, *A&A*, 303, 27
- Koopmans, L. V. E., & Treu, T. 2003, *ApJ*, 583, 606
- Koopmans, L. V. E., Treu, T., Bolton, A. S., Burles, S., & Moustakas, L. A. 2006, *ApJ*, in press (astro-ph/0601628)
- Kormann, R., Schneider, P., & Bartelmann, M. 1994, *A&A*, 284, 285
- Maoz, D., et al. 1993, *ApJ*, 409, 28
- Moré, J. J., & Wright, S. J. 1993, *SIAM Frontiers in Applied Mathematics 14: Optimization Software Guide* (Society for Industrial and Applied Mathematics)
- Morgan, N. D., Gregg, M. D., Wisotzki, L., Becker, R., Maza, J., Schechter, P. L., & White, R. L. 2003, *AJ*, 126, 696
- Oke, J. B., et al. 1995, *PASP*, 107, 375
- Pettini, M., Rix, S. A., Steidel, C. C., Adelberger, K. L., Hunt, M. P., & Shapley, A. E. 2002, *ApJ*, 569, 742
- Pindor, B., et al. 2004, *AJ*, 127, 1318
- Richards, G. T., Strauss, M. A., Pindor, B., Haiman, Z., Fan, X., Eisenstein, D., Schneider, D. P., Bahcall, N. A., Brinkmann, J., & Brunner, R. 2004, *AJ*, 127, 1305
- Santos, M. R., Ellis, R. S., Kneib, J.-P., Richard, J., & Kuijken, K. 2004, *ApJ*, 606, 683
- Seitz, S., Saglia, R. P., Bender, R., Hopp, U., Belloni, P., & Ziegler, B. 1998, *MNRAS*, 298, 945
- Shapley, A. E., Steidel, C. C., Pettini, M., & Adelberger, K. L. 2003, *ApJ*, 588, 65
- Treu, T., Koopmans, L. V. E., Bolton, A. S., Burles, S., & Moustakas, L. A. 2006, *ApJ*, in press (astro-ph/0512044)
- Warren, S. J., Hewett, P. C., Lewis, G. F., Moller, P., Iovino, A., & Shaver, P. A. 1996, *MNRAS*, 278, 139
- Willis, J. P. 2000, *The Observatory*, 120, 427
- Willis, J. P., Hewett, P. C., & Warren, S. J. 2005, *MNRAS*, 363, 1369
- Willis, J. P., Hewett, P. C., Warren, S. J., Dye, S., & Maddox, N. 2006, *MNRAS*, in press (astro-ph/0603421)
- Wisotzki, L., Schechter, P. L., Bradt, H. V., Heinmüller, J., & Reimers, D. 2002, *A&A*, 395, 17
- Yee, H. K. C., Ellingson, E., Bechtold, J., Carlberg, R. G., & Cuillandre, J.-C. 1996, *AJ*, 111, 1783
- York, D. G., et al. 2000, *AJ*, 120, 1579